

Dynamic decoherence control of a solid-state nuclear quadrupole qubit

E. Fraval, M. J. Sellars, and J. J. Longdell

Laser Physics Center, Research School of Physical Sciences and Engineering, Australian National University.

(Dated: April 6, 2019)

We report on the application of a dynamic decoherence control pulse sequence on a nuclear quadrupole transition in $\text{Pr}^{3+}:\text{Y}_2\text{SiO}_5$. Process tomography is used to analyse the effect of the pulse sequence. The pulse sequence was found to increase the decoherence time of the transition to over 30 seconds. Although the decoherence time was significantly increased, the population terms were found to rapidly decay on the application of the pulse sequence. The increase of this decay rate is attributed to inhomogeneity in the ensemble. Methods to circumvent this limit are discussed.

PACS numbers: 03.67.Pp, 76.70.Hb, 76.30.Kg, 76.60.-k, 76.70.Hb, 76.60.Lz, 76.60.Es

The use of optically active centers in solids and in particular rare-earth ions in crystals for quantum information processing shows tremendous promise. The feasibility of using rare-earth centers for quantum computing has recently been confirmed with the demonstration of one and two qubit gate operations [1, 2]. Rare-earth doped crystals also provide high optical density systems in which the participating ions are stationary for quantum optics experiments. This is important for the development of slow and stopped light [3] quantum optical memories for use in quantum cryptographic networks and optical quantum computing schemes.

Of significant interest for these applications of rare earth centers is the potential storing quantum information in the centers' ground state hyperfine transitions [4, 5]. The duration and fidelity that with which information can be stored depends on the decoherence time of the hyperfine transitions. In previous work we demonstrated that relatively long coherence times of 82ms could be achieved for the $m_I = -1/2 \leftrightarrow +3/2$ transition in $\text{Pr}^{3+}:\text{Y}_2\text{SiO}_5$ with the application of a precisely aligned, static magnetic field [6]. In this letter we demonstrate the further increase of the decoherence time of this transition through the use of a simple dynamic decoupling technique, referred to as the "Bang Bang" pulse sequence [7, 8, 9, 10]. We also investigate the effect this pulse sequence has on arbitrary initial states.

Dynamic decoupling methods for open systems were initially developed for use in NMR spectroscopy [11]. These pulse sequences are constructed such that unwanted contributions to the spin Hamiltonian can be selectively removed. The "Bang Bang" pulse sequence is designed to decouple the quantum system of interest from the bath and consists of a pair of hard pulses (δ ; δ) separated by the cycling time τ_c . This sequence minimizes the phase error accumulated due to perturbations in transition frequency resulting from changes in the environment surrounding the quantum system of interest. The Bang Bang pulse sequence can theoretically rephase all the coherence in the quantum system, thereby making $T_2 = T_1$

if the following criterion [9] is met.

$$\omega_c \tau_c \ll 1 \quad (1)$$

where ω_c is the cutoff frequency of the dephasing bath and τ_c is the period between the pulses in the Bang Bang sequence. The pulses are assumed to be "hard" such that during the pulse any evolution of the state other than the action of the driving field is assumed to be negligible. This is only truly satisfied if the pulses are arbitrarily strong and instantaneous.

For Pr ions substituting for Y in Y_2SiO_5 the main source of decoherence for the ground state hyperfine transitions is magnetic interactions with nuclei in the host [6, 12]. Y is the main component of the host that possess a nuclear spin, with a magnetic moment of $\mu_Y = 209 \mu_N$. The only other nuclear spin in the host is ^{29}Si found in natural abundance (4%) with a moment of $845 \mu_N$. The magnetic field seen by any given Pr ion fluctuates over time due to resonant cross relaxations between the host spins. The sensitivity of the Pr hyperfine transition to magnetic field fluctuations can be calculated using the reduced Hamiltonian for the electronic ground state hyperfine structure, determined by Longdell et al [2]. Pr has a nuclear spin of 5/2 and due to a pseudoquadrupole interaction its electronic ground state splits into three doubly levels with splittings of the order of 10 MHz. The near degeneracy can be lifted by a magnetic field through an enhanced nuclear Zeeman interaction. In the region where the applied field produces anticrossings a specific field direction and magnitude can be found such that there is no first order Zeeman shift for the $m_I = -1/2 \leftrightarrow +3/2$ Pr hyperfine transition [6].

Our previous work [6] showed that the dephasing perturbations acting on the Pr ions were predominantly occurring on a timescale longer than 10ms. Given that Rabi frequencies greater than 100kHz are readily achievable the period between the applied pulses in the bang bang sequence can be made such that the inequality (1) is satisfied for the dominant perturbations. A $\text{Pr}^{3+}:\text{Y}_2\text{SiO}_5$ 0.05% concentration crystal (Scientific Materials) maintained at temperature of 1.5K in a liquid helium bath cryostat was used for all the measurements. Yttrium orthosilicate (Y_2SiO_5) is a low symmetry host with two crystallographically inequivalent sites where Pr

Electronic address: elliot.fraval@anu.edu.au

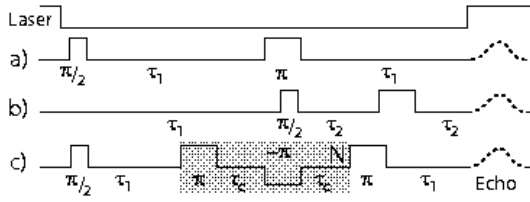


FIG. 1: Pulse sequences used in experiment: a) 2 pulse spin echo, b) Inversion Recovery T_1 c) echo pulse sequence incorporating the Bang-Bang pulse sequence iterated N times. The laser is common to all pulse sequences

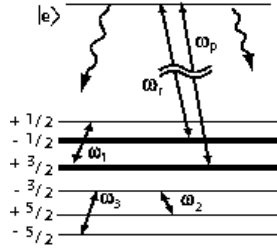


FIG. 2: All ground state hyperfine levels other than $m_I = 1=2$ interact via RF frequencies ω_{1-3} with laser radiation either at the read frequency ω_r or pump frequency ω_p . Through spontaneous emission from the common electronic excited state the group of ions interacting with both ω_r and ω_p via any common excited state will be holeburned into the $m_I = 1=2$ state. Bold states are the Critical Point transition.

can substitute for Y, labelled 'site 1' and 'site 2' [13]. Only site 1 ions are used in this work. The coordinate system chosen is the C_2 axis is y, z is the direction of polarisation of the optical $^3H_4 \rightarrow ^1D_2$ transition and x is perpendicular to both.

The magnetic fields to achieve the Critical Point field configuration ($B_{CP} = (732; 173; 219)G$ [6]) were supplied by two orthogonal superconducting magnets supplying a z field, and x/y field. The sample was rotated about the z axis to provide the correct ratio of fields along the x and y axes for the critical point in magnetic field space. The field in the x/y plane could also be adjusted using a small correction coil mounted orthogonal to the main x/y. The inhomogeneity in magnetic field across the sample was measured using a hall probe to be $< 2G$ in the z direction. The frequency of the $m_I = 1=2 \rightarrow +3=2$ ground state hyperfine transition at the Critical Point field was $8.646 MHz$.

Raman heterodyne was employed to investigate the ground state hyperfine transitions using an experimental setup similar to that described in previous work [6]. The experiment was performed using a Coherent 699 frequency stabilized tunable dye laser tuned to the $^3H_4 \rightarrow ^1D_2$ transition at $605.977nm$. The laser's frequency was stabilized to a sub-kilohertz linewidth. The laser power incident on the crystal was $40mW$, focused to $100\mu m$ and could be gated using a $100MHz$ acousto-optic modulator. The hyperfine transition was excited using a six turn

coil with a diameter of $5mm$, driven by a $10W$ RF amplifier resulting in a Rabi frequency $\omega_{RF} = 91kHz$. The RF pulse and digital control sequences were generated using a direct digital synthesis system (manufacture by SpinCore) referenced to an oven controlled crystal oscillator. The pulse sequences used in the experiment are illustrated in 1. The Raman heterodyne signal, seen as a beat on the optical beam, was detected by a $125MHz$ NewFocus photodiode. This signal was analyzed using a mixer and a phase controlled local oscillator referenced to the RF driving field.

At the Critical Point field the $m_I = 1=2 \rightarrow +3=2$ transition was observed at $8.646MHz$ with a inhomogeneous linewidth of $4kHz$. This linewidth was found to be insensitive to changes in the magnetic field of the order of $10G$.

Prior to applying each Raman heterodyne pulse sequence the sample was prepared with the optical/RF repump scheme as shown in figure 2. The repump frequencies were $\omega_r = \omega_p = 18.2MHz$, $\omega_1 = 12.2$, $\omega_2 = 15.35MHz$ and $\omega_3 = 16.3MHz$. The repump RF was pulsed with a duty cycle of 10% to reduce sample heating, while the repump laser frequency ω_r was scanned $200kHz$ to holeburn a trench in the inhomogeneous optical line where detection would take place. This repump scheme ensures that all P rions interacting with the laser radiation are forced into the $m_I = 1=2$ state, creating a pure state ensemble. It also ensures there is no initial population near the laser frequency used for Raman Heterodyne detection. The use of a sub-kilohertz linewidth laser and the repump scheme resulted in a significant improvement in the signal to noise compared to work performed earlier [6].

Figure 3 shows the decay of the amplitude of two pulse spin echoes as a function of the delay between the pulses. Two data sets are shown; the first is for an applied magnetic field optimized for long decay times and the second for a field detuned by $5G$ in the z direction from the optimal value. The significantly longer decay time for the optimized field in the present work, compared to previous work [6] is attributed to the addition of the correction coil enabling significantly more precise magnetic field adjustments. Besides being longer the decay can no longer be described by standard echo decay function with a single time constant [14]. There are three distinct regions. For pulse separations less than $20ms$ the decay rate is less than $1=4s^{-1}$. At $30ms$ there is a distinct shoulder with the decay rate increasing to $1=0.4s^{-1}$ as the pulse separation reaches $60ms$. From $150ms$ onwards the decay rate asymptotically approaches a value of $1=0.86s^{-1}$. This asymptotic decrease in the decay rate was only observed for magnetic fields within $0.5G$ of the optimal field.

The shoulder in the decay at $30ms$ indicates that the majority of the dephasing is due to perturbations that occur on time scales between 10 and $100ms$. The asymptotic behavior of the decay is attributed to a variation in the T_2 within the ensemble resulting from inhomogeneity in the magnetic field across the sample. Ions experiencing

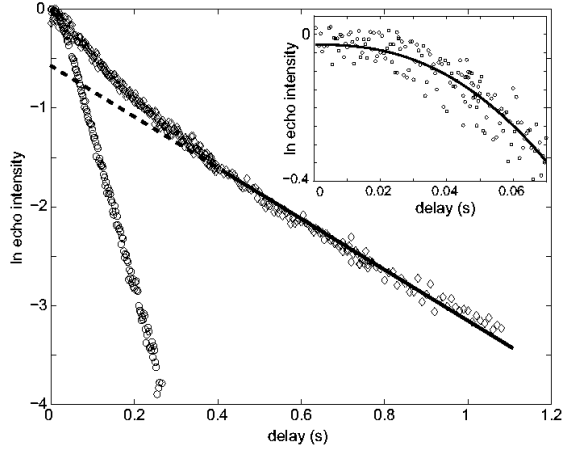


FIG. 3: Spin echo decay at the Critical Point (○), and detuned from the Critical Point (□) by 5G in the z direction (○).

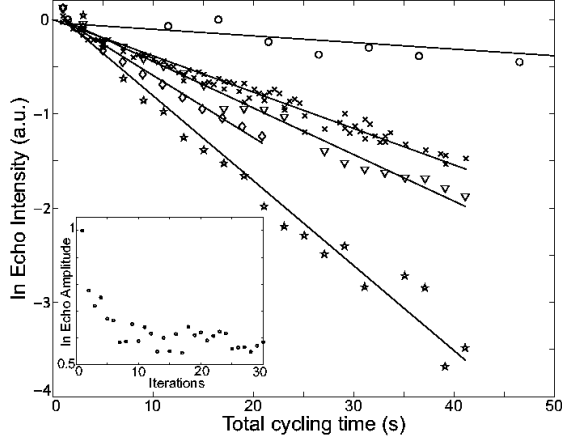


FIG. 4: Bang Bang decoupled echo decays with $\tau_c = 7.5\text{ms}$ (○); 10ms (□); 15ms (△); 20ms (◇) corresponding to $T_2 = 27.9; 21.1; 15.2; 10.9\text{s}$. Inversion recovery measurements (○) yield $T_1 = 145\text{s}$.

a field closer to the Critical Point will have a longer T_2 and consequently their contribution to the echo intensity will dominate for long pulse separations. The asymptotic decay rate gives a lower limit for the total second order magnetic broadening of the transition of 1.15H z .

The Bang Bang pulse sequence was investigated using an initial delay of $\tau_1 = 1.2\text{ms}$ and varying the cycling time τ_c from 20ms to 0.5ms , as shown in figure 4. Also shown in figure 4 is the result of an inversion recovery measurement used to determine the lifetime of the transition. To determine the upper limit of T_2 , which is T_1 , inversion recovery measurements were performed as described in figure 1 and are shown in figure 4. As shown in figure 4 the Bang Bang sequence significantly increases T_2 .

In figure 5 the coherence times T_2 for each of the data sets are plotted as a function of the cycling time τ_c . This shows that for $\tau_c < 5\text{ms}$, there are significant gains

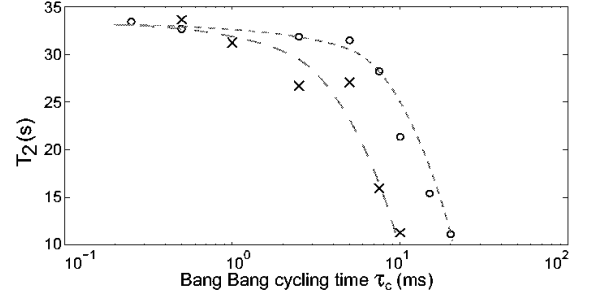


FIG. 5: Dependence of decoherence time on the Bang Bang cycling time τ_c both at the critical point (○) and with the magnetic field misaligned to give a coherence time of $T_2 = 100\text{ms}$ (×). Trend lines are included but do not represent a physical model.

in T_2 made by reducing τ_c , while reducing τ_c further only slightly increases in T_2 . In order to investigate the origin of this plateau the magnetic field was detuned from the Critical Point to achieve an undriven T_2 of 100ms for a two pulse echo measurement (see figure 3), significantly increasing the sensitivity of the Proton hyperfine transition to magnetic field fluctuations. It is clear that there is a significant reduction in T_2 for the same τ_c when detuned from the critical point, consistent with increased sensitivity to magnetic dephasing sources. The difference in T_2 reduces over the plateau region until they are both approximately 33 seconds at $\tau_c = 250\text{s}$. If the limit of T_2 for short τ_c was due to magnetic field fluctuations, detuning from the Critical Point should lower the value to which T_2 asymptotes towards. That this does not appear to be the case indicates that the 33 second limit is not due to magnetic interactions. Possible limitations are a non-magnetic dephasing mechanism becoming significant or that the fidelity of applied pulses now limits T_2 . To assess how well an arbitrary quantum state was preserved by the Bang Bang pulse sequence we performed process tomography on the input state and for 1, 10, 100 and 1000 iterations of the Bang Bang cycle. The initial delay was $\tau_1 = 1.2\text{ms}$, with a cycling time of $\tau_c = 2\text{ms}$. The total period over which the tomography is performed is 4ms , 40ms , 400ms and 4s respectively. The imaginary component of the process tomography is only shown for the input state since it never contributed more than 10% of the signal. Ideally the Bang Bang process operator is the identity matrix, leaving the state unchanged. What was observed was that the component of the Bloch vector in the coherence plane for a given state was preserved well, while the population component of the Bloch vector rapidly decayed. The fidelity of the Bang Bang process for 1, 10, 100 and 1000 iterations was 99%, 65%, 54% and 43% respectively.

The evolution of the ensemble was modelled using the Bloch equations assuming an infinite T_1 and T_2 , with an inhomogeneous linewidth of 4kHz (FWHM) and a Rabi frequency of 100kHz . The results from this modelling are shown in figure 6, alongside the experimental data. De-

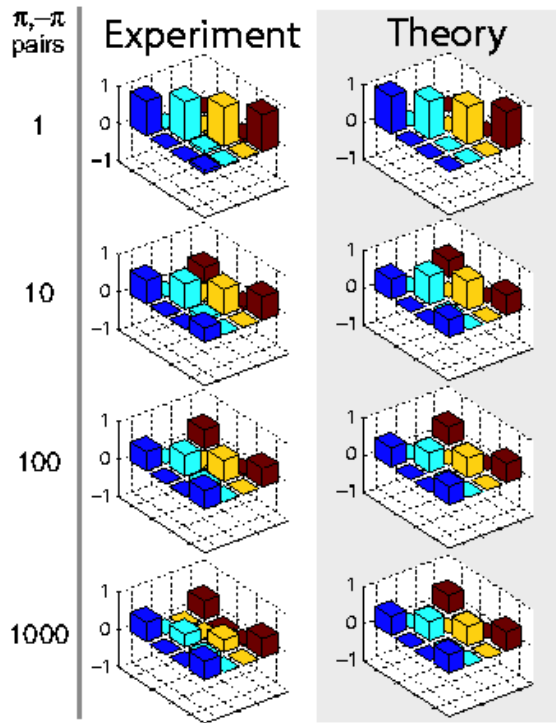


FIG. 6: Process tomography of the Bang Bang pulse sequence for 1, 10, 100 and 1000 iterations for both experiment and theoretical modelling. The imaginary component of both the experiment and modelling is always zero and is omitted for clarity.

spite the model not including any homogeneous dephasing the main features of the simulated process tomography (figure 6) closely matches those of the experimental data. In particular the rapid decay of the population component of the Bloch vector compared to the coherence components. Further simulations indicated that the decay rate of the population terms can be reduced by increasing the ratio of the Rabi frequency to the linewidth. A suitable criteria for when the application of the Bang Bang pulse sequence is useful for preserving arbitrary

quantum states is when the decay rate of the population terms in the presence of the pulse sequence is slower than that of the coherence terms in the absence of the sequence. For the present case where $T_2 = 0.86$ s the simulation indicates that to meet this criteria it will be necessary to achieve a ratio of Rabi frequency to linewidth of $\omega_{RF} = \omega_{inh} / 100$. There is limited capacity to increase the Rabi frequency of the driving field without the possible excitation of off-resonant transitions. Therefore for the application of the Bang Bang pulse sequence to the $m_I = -1/2 \rightarrow 3/2$ transition to be useful it will be necessary to reduce the inhomogeneous broadening of the transition by a factor of 10.

The large change in magnetic field sensitivity as the Critical Point field is approached with no corresponding change in the inhomogeneous linewidth of the transition suggests that the inhomogeneous broadening of the transition at the Critical Point field is not due to magnetic interactions. The inhomogeneous broadening at the Critical Point field is probably due to strain within the crystal and not intrinsic to the site, which can be reduced by refining standard crystal growing techniques. While a reduction in strain broadening by over an order of magnitude has been achieved in analogous materials [15] through reducing the dopant concentration, though we cannot predict the limit for $\text{Pr}^{3+}:\text{Y}_2\text{SiO}_5$. Irrespective of reaching the desired ratio of Rabi frequency to inhomogeneous linewidth, pulse sequences more robust to Rabi and detuning errors have been proposed [16, 17].

In conclusion the application of the Bang Bang pulse sequence demonstrates that dynamic decoupling techniques are applicable to correcting quantum errors on nuclear spin transitions of $\text{Pr}^{3+}:\text{Y}_2\text{SiO}_5$. We have stored arbitrarily phased nuclear spin superposition states for over 30 s in $\text{Pr}^{3+}:\text{Y}_2\text{SiO}_5$. This system is the first solid state quantum computing candidate to preserve phase information for periods comparable to liquid phase NMR or trapped atom implementations.

The support of this work by the Defence Science Technology Organisation (DSTO) and the Australian Research Council (ARC) is gratefully acknowledged.

-
- [1] J. J. Longdell and M. J. Sellars, Phys. Rev. A 69, 032307 (2004).
 - [2] J. J. Longdell, M. J. Sellars, and N. B. Manson, Phys. Rev. B 66, 035101 (2002).
 - [3] A. V. Tunukin, V. S. Sudarshanam, M. S. Shahrier, J. A. Musser, B. S. Ham, and P. R. Hemmer, Phys. Rev. Lett. 88, 023602 (2002).
 - [4] N. Ohlsson, R. K. M. Chan, and S. Kroll, Optics Comm. 201, 71 (2002).
 - [5] S. A. Moiseev and S. Kroll, Phys. Rev. Lett. 87, 173601 (2001).
 - [6] E. Fraval, M. Sellars, and J. J. Longdell, Phys. Rev. Lett. 92, 077601 (2004).
 - [7] L. Viola, Advances in decoherence control (2004), quant-ph/0404038.
 - [8] M. S. Byrd and D. A. Lidar, Phys. Rev. Lett. 89, 047901 (2002).
 - [9] L. Viola and S. Lloyd, Phys. Rev. A 58, 2733 (1998).
 - [10] D. Vitali and P. Tombesi, Phys. Rev. A 59, 4178 (1999).
 - [11] E. L. Hahn, Phys. Rev. 80, 580 (1950).
 - [12] E. Fraval, M. J. Sellars, A. Morrison, and A. Ferris, J. Lum. 107, 347 (2004).
 - [13] R. W. E. Quall, R. L. Cone, and R. M. Macfarlane, Phys. Rev. B 52, 3963 (1995).
 - [14] W. B. Mims, Phys. Rev. 168, 370 (1968).
 - [15] R. M. Macfarlane, R. S. Meltzer, and B. Z. Malkin, Phys. Rev. B 58, 5692 (1998).
 - [16] L. Viola and E. Knill, Phys. Rev. Lett. 90, 037901 (2003).
 - [17] P. Wojcik, (2004), quant-ph/0410107.